Molecular Cell, Vol. 11, 807–815, March, 2003, Copyright ©2003 by Cell Press

Failure to Produce Mitochondrial DNA Results in Embryonic Lethality in *Rnaseh1* Null Mice

Susana M. Cerritelli,[1] Ella G. Frolova,[2] Chiguang Feng,[2] Alexander Grinberg,[2] Paul E. Love,[2] and Robert J. Crouch[1,*]
[1]Laboratory of Molecular Genetics
[2]Laboratory of Mammalian Genes and Development
National Institute of Child Health and Human Development
National Institutes of Health
Bethesda, Maryland 20892

Summary

Although ribonucleases H (RNases H) have long been implicated in DNA metabolism, they are not required for viability in prokaryotes or unicellular eukaryotes. We generated *Rnaseh1*$^{-/-}$ mice to investigate the role of RNase H1 in mammals and observed developmental arrest at E8.5 in null embryos. A fraction of the mainly nuclear RNase H1 was targeted to mitochondria, and its absence in embryos resulted in a significant decrease in mitochondrial DNA content, leading to apoptotic cell death. This report links RNase H1 to generation of mitochondrial DNA, providing direct support for the strand-coupled mechanism of mitochondrial DNA replication. These findings also have important implications for therapy of mitochondrial dysfunctions and drug development for the structurally related RNase H of HIV.

Introduction

For many years, the prevailing model for replication of mitochondrial DNA (mtDNA) has invoked a strand-asymmetric mechanism of duplication, with two origins of replication, one on each of the two strands of the circular mtDNA molecule (Clayton, 1982). Transcription of the mtDNA near the origin of the first-replicating strand can lead to the formation of an RNA-DNA hybrid that is processed to serve as primer for DNA replication by DNA polymerase γ (Shadel, 1999). Mitochondrial replication protein (MRP) has been implicated in formation of the RNA primer(s) (Lee and Clayton, 1997, 1998). Replication then proceeds by copying along one strand until the displacement of the DNA exposes a new site in the complementary strand to be used as initiation for replication of the second strand. In 2000, Holt and colleagues reported observations that suggested mtDNA replication also follows a more classical strand-coupled mechanism (Holt et al., 2000). Further studies, using highly purified mitochondrial preparations, found numerous RNA-DNA hybrid regions in replicating mtDNA molecules (Yang et al., 2002) rather than the previously reported single-stranded DNA intermediates associated with the asymmetric mechanism. These results have been interpreted to indicate that mtDNA replication proceeds mainly by the classic coupled leading-lagging-strand mode of DNA synthesis and that the RNA-DNA hybrids are RNA primers of DNA replication. The presence of abundant RNA-DNA hybrids in replicating mtDNA suggests the participation of one or more proteins with ribonuclease H activity for proper formation of mature mtDNA.

Since their discovery (Stein and Hausen, 1969), RNases H have been suggested to be involved in removing the RNA of RNA-DNA hybrids (Crouch and Toulmé, 1998), particularly the primers of Okazaki fragments in lagging-strand DNA synthesis (Kogoma and Foster, 1998). Two additional, seemingly contradictory, functions of RNase HI have been described. One is to generate primers for initiation of DNA replication (Dasgupta et al., 1987), and the second is to eliminate, in a general manner, RNA-DNA hybrids, some of which in *Escherichia coli* can serve as primers at sites other than oriC, the normal origin of replication (de Massy et al., 1984). Neither of these functions is essential for cell viability in *E. coli* (Itaya et al., 1999) or *Saccharomyces cerevisiae* (Arudchandran et al., 2000; Frank et al., 1998b), indicating other means of resolution of these structures. In contrast, the RNase H of the retroviral reverse transcriptase is absolutely necessary for generating primers for DNA replication and removal of the genomic viral RNA once it has been reverse transcribed (Hughes et al., 1998).

Studies have shown that RNase H1 is present in nuclei (Frank et al., 1998a; ten Asbroek et al., 2002), as would be expected for a protein involved in DNA replication and repair. However, RNase H1 has also been isolated from mitochondria of *Neurospora crassa* (Wang and Lambowitz, 1993), beef heart (Pileur et al., 2000), and *Xenopus laevis* oocytes (Cazenave et al., 1994), and there is strong evidence that RNase H1 is present in both mitochondria and nuclei of *Crithidia fasciculata* (Engel et al., 2001). However, deletion of the *RNH1* gene in *C. fasciculata* (Ray and Hines, 1995) or in *S. cerevisiae* (Arudchandran et al., 2000) does not lead to loss of mitochondrial function.

Mouse and human RNases H1 have an amino acid sequence at their N termini, absent in a number of other eukaryotic RNases H1 including *S. cerevisiae*, with characteristics of a mitochondrial localization signal. In this report, we demonstrate that the N-terminal extension present in mammalian RNases H1 is able to target the protein to mitochondria. Moreover, mice deleted for the *Rnaseh1* gene arrest development about day E8.5 because of a failure to generate mtDNA, indicating an essential role for RNase H1 during mammalian embryogenesis.

Results

Characterization and Disruption of the *Rnaseh1* Gene

Eukaryotic RNases H1 belong to a widespread family of ribonucleases with members in most prokaryotes, eukaryotes, and LTR-retroviruses (Crouch and Toulmé, 1998). Some of these RNases H are multifunctional pro-

*Correspondence: robert_crouch@nih.gov

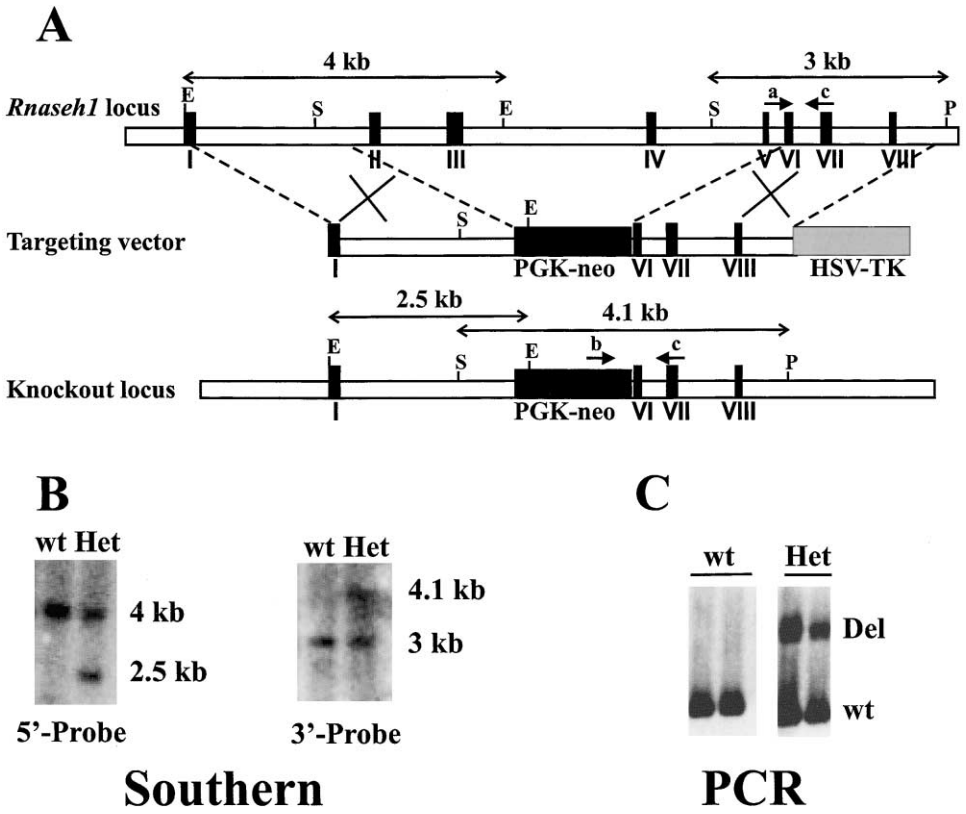

Figure 1. Disruption of the *Rnaseh1* Gene

(A) Schematic representation of wild-type, targeted *Rnaseh1* alleles, and the gene-targeting construct. Black rectangles and roman numerals represent exons. A black box depicts the neomycin resistance cassette (PGK-neo), and a gray rectangle the thymidine kinase marker (HSV-TK). Arrow "a" represents the oligonucleotide primer specific for the *Rnaseh1*$^{+}$ allele, arrow "b" the *Rnaseh1*$^{-}$ allele, and arrow "c" a common primer for both the *Rnaseh1*$^{+}$ and *Rnaseh1*$^{-}$ alleles. E, EaeI; P, PsiI; and S, SspI are restriction enzyme sites.

(B) Identification of heterozygous-targeted embryonic stem (ES) cell clones. ES-cell DNA was digested with EaeI, or with SspI-PsiI, and analyzed by Southern blotting using oligonucleotide probes of about 50 bases corresponding to the *Rnaseh1* gene outside the sequences included in the targeting vector.

(C) Genotyping of the *Rnaseh1* locus by multiplex PCR. Adult mice were genotyped by PCR with three different primers a, b, and c as described above. "Del" and "wt" indicate PCR products amplified from the *Rnaseh1*$^{-}$ and *Rnaseh1*$^{+}$ alleles, respectively.

teins containing additional domains. The RNase H region of the eukaryotic protein is attached to a highly conserved duplex-RNA binding domain by a connecting sequence of variable length and amino acid composition (Crouch et al., 2001). The function of the non-RNase region and the reason of its association with the RNase H domain are unknown. To better understand the role of RNase H1 in eukaryotes, we generated *Rnaseh1*$^{-/-}$ mutant mice by gene targeting. We obtained BAC clones by hybridization of mouse *Rnaseh1* cDNA with a mouse ES BAC DNA library (Cerritelli and Crouch, 1998), and the sequence of the *Rnaseh1* gene was determined. The complete sequence of the genomic region containing the *Rnaseh1* gene appeared in GenBank (>lcl|Mm12_WIFeb01_232) during the course of the work described here. The gene is about 9.5 kb in length and comprises 8 exons and 7 introns, the latter ranging in size from about 0.3–2.3 kb (Figure 1A). It has a 500 bp 3′-UTR sequence.

We replaced four of eight exons of the *Rnaseh1* gene by a neomycin resistance cassette (Figure 1A), deleting coding regions for both activities of the protein. Three ES cell clones with the targeted *Rnaseh1* allele were obtained, as determined by Southern analysis, and heterozygous mice were generated. Genotypes were ascribed by Southern analysis (Figure 1B), PCR assays (Figure 1C), and partial DNA sequence determination (data not shown).

Loss of RNase H1 Causes Embryonic Lethality

Mice heterozygous for the targeted allele *Rnaseh1*$^{+/-}$ were viable and fertile and exhibited no obvious phenotypic abnormalities. However, no *Rnaseh1*$^{-/-}$ mice were obtained from intercrosses of heterozygous mice. Genotyping of staged embryos showed that death occurs by mid-gestation with only resorbed *Rnaseh1*$^{-/-}$ embryos at E10.5 (Table 1). The 85 embryos examined at day 9.5

Table 1. Genotyping of Newborn Pups and Staged Embryos

Stage	Total	+/+	+−	−/−
Newborn	103	36	67	0
E10.5	10	4	10	6[a]
E9.5	85	18	44	23
E8.5	33	8	16	9

[a] Resorbed embryos.

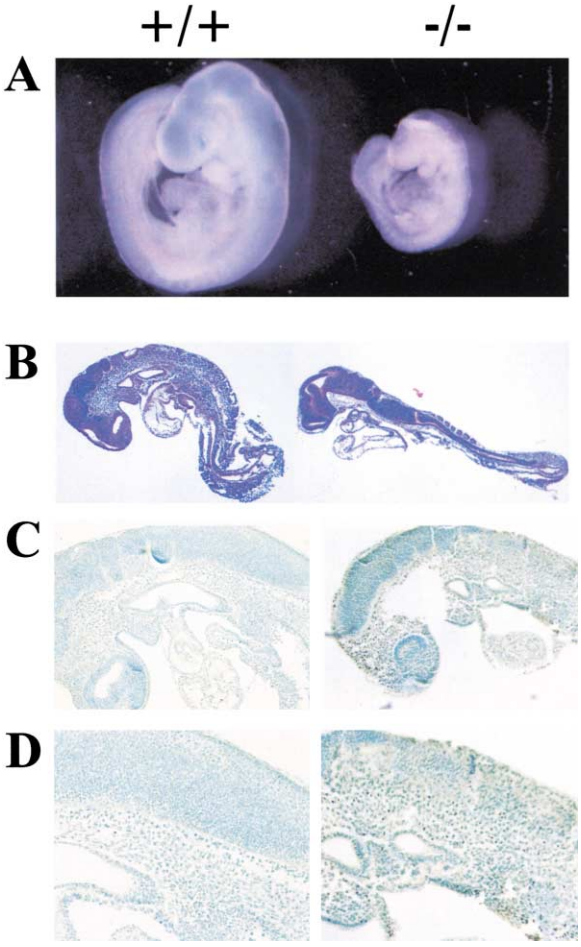

Figure 2. Morphology of *Rnaseh1*$^{-/-}$ Embryos

(A) Gross morphology of embryos representing *Rnaseh1*$^{+/+}$ and *Rnaseh1*$^{-/-}$ littermates at day 9.5 postcoitum (E9.5).

(B) Histological sections of embryos from *Rnaseh1*$^{+/+}$ and *Rnaseh1*$^{-/-}$ littermates at E9.5 stained with hematoxylin and eosin. Approximate gestational ages (± 0.5 days) were estimated from vaginal plug dates.

(C) TUNEL staining of E9.5 embryos shows abundant TUNEL-positive cells in *Rnaseh1*$^{-/-}$ but not in control littermate.

(D) 2× magnification of (C) to demonstrate abundance of TUNEL-positive cells in the null embryo.

postcoitum (E9.5) showed a Mendelian distribution of the three possible genotypes. However, *Rnaseh1*$^{-/-}$ embryos were developmentally delayed and considerably smaller than wild-type or heterozygous littermates (Figure 2A). Histological sections and microscopic inspection revealed no gross morphological defects (Figure 2B), indicating that *Rnaseh1*$^{-/-}$ embryos develop normally until approximately day 8.5 of gestation at which point they failed to increase in size and by E10.5 were mostly resorbed.

Rnaseh1$^{-/-}$ Embryos Have Decreased mtDNA Content

Because RNase H1 has been implicated in DNA replication and repair, we examined the amount of DNA in *Rnaseh1*$^{-/-}$ embryos in an attempt to relate embryonic lethality in the absence of RNase H1 to DNA content. We compared DNA in mutant and control embryos at different days postcoitum using quantitative PCR. Total chromosomal DNA content was similar in wild-type and *Rnaseh1*$^{-/-}$ embryos until E8.5. By E9.5, null embryos contained only 10% of the DNA present in wild-type or heterozygous embryos, perhaps reflecting the size differences at this stage (Figure 2A). In contrast, the amount of mtDNA in *Rnaseh1*$^{-/-}$ embryos was already decreased at E7.5 when they were still growing and, apparently, developing normally. By E8.5, the quantity of mtDNA in homozygous null embryos was reduced to about 1% of the wild-type, and by E9.5 was less than 0.05% (Figure 3), suggesting an association between absence of mtDNA and embryonic lethality. The relative decrease of mtDNA observed in embryos defective in RNase H1 indicated that while chromosomal DNA replication continued normally, mtDNA replication was absolutely dependent on RNase H1.

We considered the possibility that any embryo becoming lethal at midgestation would show low levels of mtDNA. To test this hypothesis, we measured the amount of mtDNA present in *Ldb1*$^{-/-}$ embryos that arrest development at E7.5 (Mukhopadhyay et al., 2003) and found normal quantities of mtDNA. Therefore, loss of mtDNA in RNase H1-deficient embryos is not a general phenomenon of embryonic lethality at this stage of development.

Rnaseh1$^{-/-}$ Embryos Have Defective Mitochondria

Defective mitochondria in *Rnaseh1*$^{-/-}$ embryos were observed by enzyme histochemical analysis of respiratory chain function and by electron microscopy (EM). Enzyme histochemical staining showed an absence of mitochondrial encoded cytochrome c oxidase activity in E9.5 *Rnaseh1*$^{-/-}$ embryos, indicating severe mitochondrial dysfunction resulting from the absence of mtDNA. However, the activity of the succinate dehydrogenase, derived from a nuclear-encoded gene, was normal in both mutant and wild-type embryos (Figure 4). Electron micrographs of E9.5 *Rnaseh1*$^{-/-}$ embryos showed a heterogeneous population of abnormal mitochondria, most of which were enlarged, vacuolated, with disorganized cristae, some resembling immature organelles (Figures 5B and 5C).

Homozygous *Rnaseh1* Knockouts Show Massive Apoptosis at E9.5

Mitochondria are key regulators of the process of programmed cell death, or apoptosis. Massive in vivo apoptosis has been shown to occur in respiratory chain-deficient mouse cells lacking mtDNA (Wang et al., 2001). Because embryos with homozygous disruption of the *Rnaseh1* gene lack mtDNA and, consequently, have a severe mitochondrial dysfunction, we examined *Rnaseh1*$^{-/-}$ embryos for indications of apoptotic cell death. EM micrographs of mutant E9.5 embryos revealed a large number of cells that appeared to be undergoing apoptosis compared to wild-type age-matched embryos (Figure 5A). Mutant cells were loosely connected, with numerous apoptotic bodies. Mitochondria showing the characteristic changes associated with apoptosis were ubiquitously present (Figures 5B and 5C). To confirm apoptotic cell death, we also performed

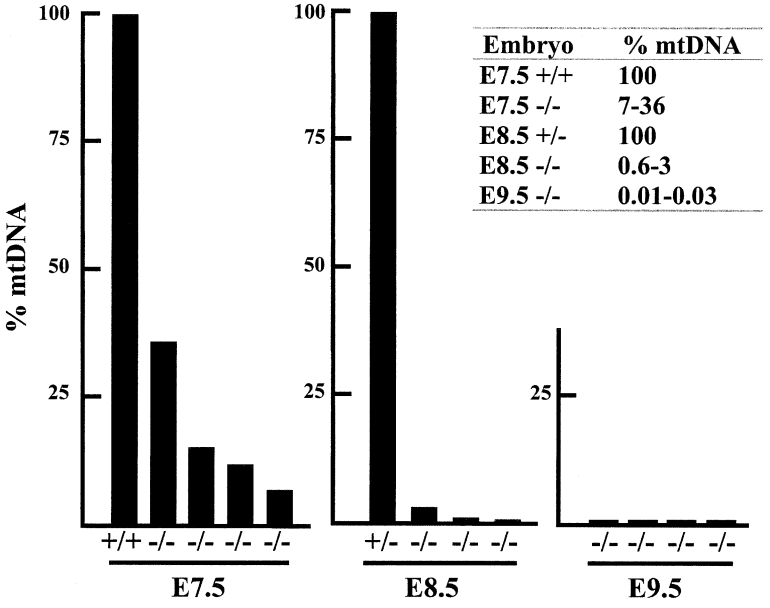

Embryo	% mtDNA
E7.5 +/+	100
E7.5 -/-	7-36
E8.5 +/-	100
E8.5 -/-	0.6-3
E9.5 -/-	0.01-0.03

Figure 3. Percentage of Mitochondrial DNA Present in *Rnaseh1* Null Mutants

The amount of mitochondrial and chromosomal DNA was estimated for embryos at E7.5, E8.5, and E9.5. The percentage of mitochondrial DNA present in mutant embryos was determined from a calibration curve constructed from serial dilutions of wild-type DNA from age-matched embryos and normalized to the amount of chromosomal DNA obtained in the same way. The graph shows independent experiments, and the table summarizes individual values.

TUNEL assays on embryos at different stages and observed abundant TUNEL-positive cells at E9.5 (Figures 2C and 2D). However, only a slight increase in TUNEL-positive cells was observed at E8.5 (data not shown), indicating that about 2 days after mtDNA content started to decrease, the absence of mitochondrial function leads to apoptosis. Other mtDNA replication-deficient mutants (Wang et al., 2001) undergo apoptosis around the same embryonic stage.

RNase H1 Localizes to the Nucleus and the Mitochondria

RNase H1, a nuclear-encoded enzyme, would need to be transported to mitochondria to have a direct effect in these organelles. RNase H1 is abundant in nuclei, but it also has been detected in mitochondria of *C. fasciculata* (Engel et al., 2001) and has been purified from mitochondria of different organisms (Cazenave et al., 1994). Mouse *Rnaseh1* transcripts have two potential in-frame AUG initiation codons, an organization typical of mRNAs encoding proteins targeted to mitochondria and another cellular compartment (Lakshmipathy and Campbell, 1999; Slusher et al., 1991; Valgardsdottir et al., 2001). The 26 amino acid sequence residing between the two AUGs was predicted by a computer algorithm (Nakai and Horton, 1999) to be a mitochondrial localization signal (MLS) (Figure 6A). To determine subcellular localization, we made a construct in which the putative MLS was fused to the GFP protein. Confocal microscopy analysis of Cos-1 or HeLa cells transiently transfected with this plasmid demonstrated that the first 26 amino acid residues of RNase H1 effectively targeted GFP to mitochondria in both monkey and human cell lines (Figures 6C and 6F). The full-length RNase H1 fused to the GFP localized to the nucleus and mitochondria, with the strongest signal in the nucleus (Figure 6G). When we removed the MLS, the protein was exclusively nuclear (Figure 6H). Subcellular partitioning of RNase H1 was similar to that of other proteins that interact with nucleic acids in both mitochondria and nuclei (Wang et al., 2002; Lakshmipathy and Campbell, 1999; Valgardsdottir et al., 2001).

Discussion

Data reported here identify a crucial role for RNase H1 in mouse development and suggest that embryonic lethality in *Rnaseh1* null mutants results from failure to replicate mtDNA. These results were surprising because deletion of the gene encoding RNase H1 in a wide variety of unicellular eukaryotes did not lead to cell death or loss of mitochondrial function (Ray and Hines, 1995; Arudchandran et al., 2000). It was also a surprise to find that *Rnaseh1*$^{-/-}$ embryos failed to produce new mtDNA. Clues that led us to examine defects in mitochondria were the timing of embryonic lethality and the presence of a putative mitochondrial localization signal at the amino termini of both mouse and human RNase H1.

During development, replication of mtDNA begins some time after implantation (Pikó and Taylor, 1987; Pikó and Matsumoto, 1977; Ebert et al., 1988), when multiple rounds of cell division have diluted the approximately 100,000 mtDNA molecules contributed at fertilization by the maternal oocyte (Steuerwald et al., 2000). In contrast, chromosomal DNA replication commences almost immediately after fertilization. Our data show that at E7.5 the amount of mtDNA in *Rnaseh1*$^{-/-}$ embryos was about 10% of that present in the wild-type embryos and decreased further to 1% at E8.5 and 0.05% at E9.5. The relative decrease of mtDNA observed in *Rnaseh1*$^{-/-}$ embryos as development progresses implies that, in the absence of RNase H1, maternally inherited mtDNA is diluted to very low levels, because there is no new synthesis, while chromosomal DNA content increases due to normal replication.

Until the early blastocyst stage, maternally derived mitochondria and the use of lactate to generate ATP obviate the need for newly formed mitochondria (Ginsberg and Hillman, 1973). Mice unable to produce func-

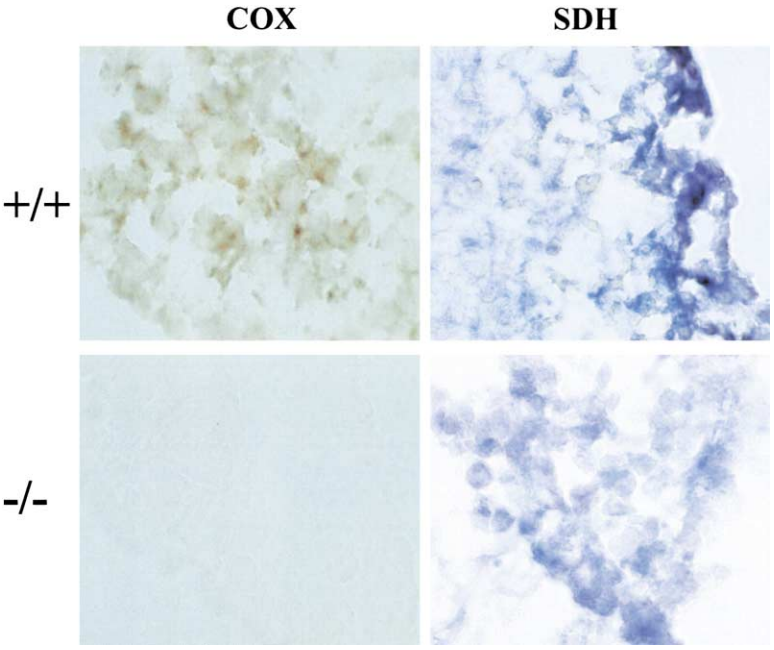

Figure 4. Enzyme Histochemical Analysis of Respiratory Chain Function in Homozygous *Rnaseh1* Mutant and Wild-Type Embryos

Enzyme histochemical staining for cytochrome c oxidase (COX) and succinate-dehydrogenase (SDH) activities was performed on tissue sections from wild-type (+/+) and homozygous mutant (−/−) E9.5 embryos.

tional mitochondria, including *Rnaseh1*$^{-/-}$, arrest development around E8.5 (Larsson et al., 1998; Li et al., 2000) and when cytochrome c is present undergo apoptotic cell death (Wang et al., 2001). At this stage, rapid mitochondrial replenishment is crucial, as embryos begin to depend on oxidative phosphorylation for energy production. In *Xenopus laevis* embryos, mtDNA replication begins at the heartbeat stage (Chase and Dawid, 1972), emphasizing the need for mature mitochondria at the time the circulatory system becomes available.

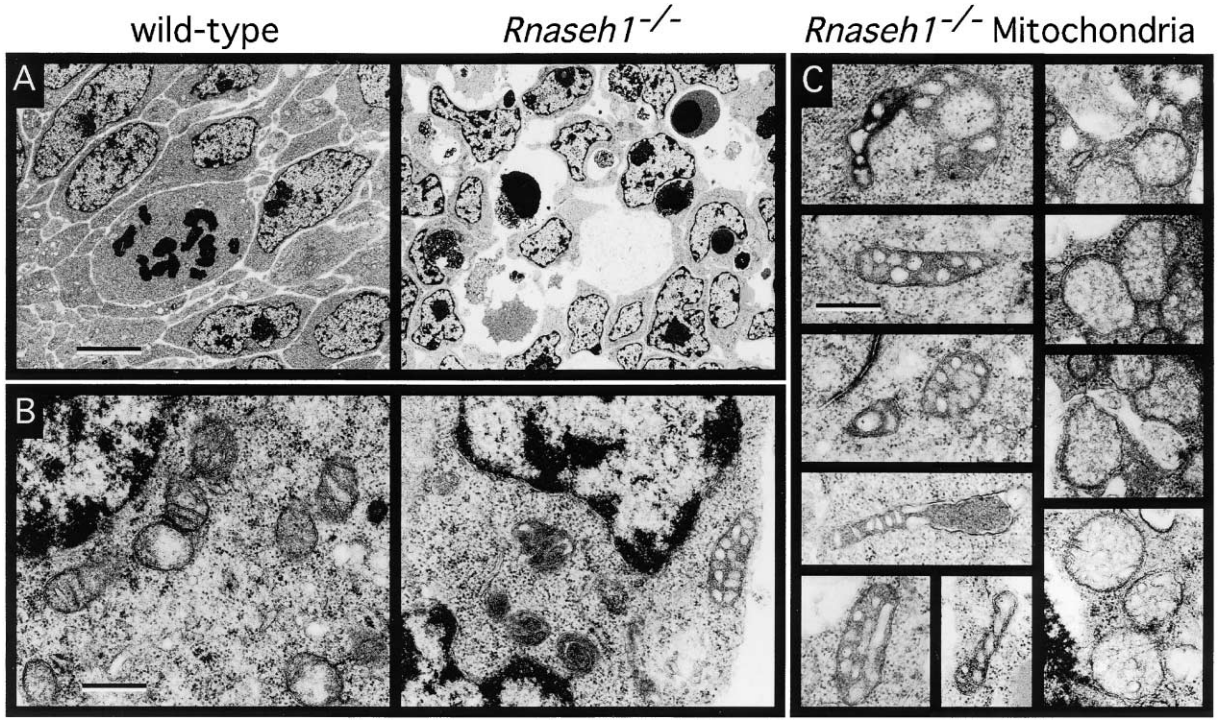

Figure 5. Cellular and Mitochondrial Morphology in Wild-Type and *Rnaseh1*$^{-/-}$ E9.5 Embryos

(A) Electron micrograph of tissue sections from wild-type and *Rnaseh1*$^{-/-}$ E9.5 embryos. The scale bar represents 5 microns.

(B) Electron micrograph of tissue sections from wild-type and *Rnaseh1*$^{-/-}$ E9.5 embryos, at higher magnification, showing mitochondrial details. The scale bar represents 0.5 microns.

(C) Several examples of abnormal mitochondria observed in *Rnaseh1*$^{-/-}$ E9.5 embryos by EM. The scale bar represents 0.5 microns.

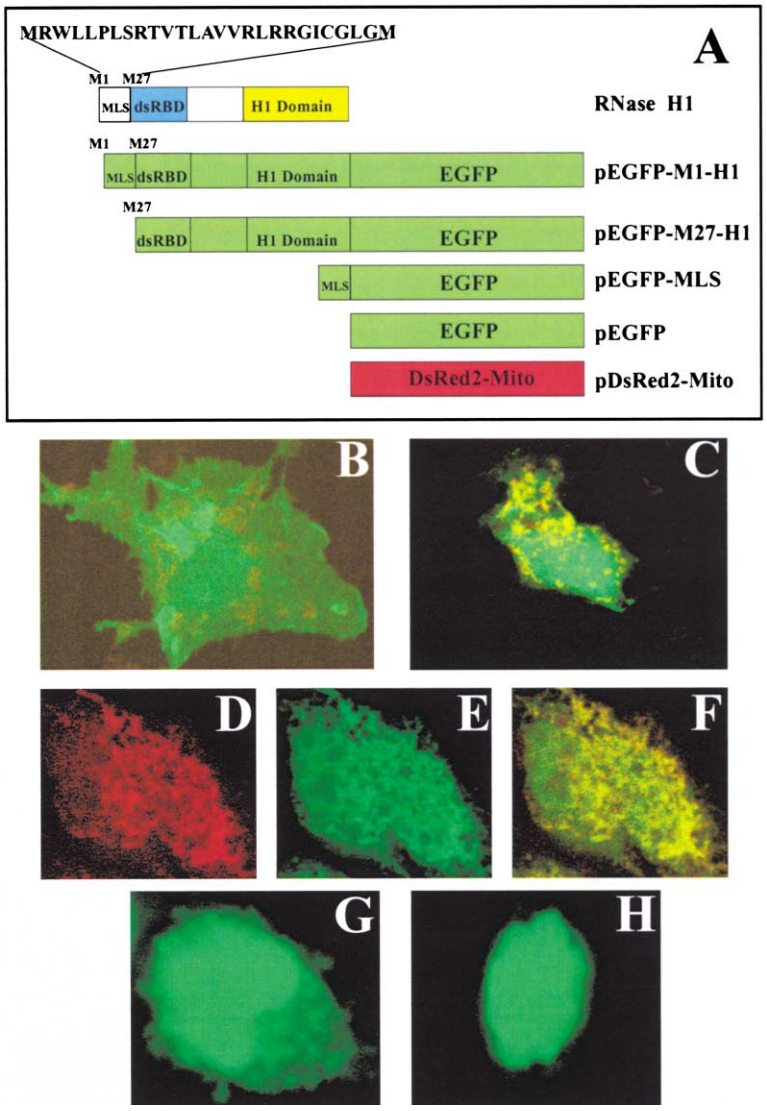

Figure 6. Subcellular Localization of RNase H1-GFP Fusion Proteins

(A) RNase H1-GFP fusion constructs. RNase H1 is schematically represented with the RNase H domain in yellow and the double-stranded RNA binding domain in blue. The sequence for the mitochondrial localization signal (MLS) is shown on top. pEGFP-M1-H1 represent the fusion of the RNase H1 and the GFP coding sequence. In pEGFP-M27-H1, the RNase H1 protein starts at M27. The pEGFP-MLS construct has the first 26 amino acid sequence of the RNase H1 protein attached to the GFP sequence. pEGFP is the green fluorescent protein encoded in the plasmid pEGFP-N2 (Clontech), and pDsRed2-Mito represents the red fluorescent protein encoded in the vector pDsRed2-Mito (Clontech).

(B) Cos-1 cells were transiently transfected with pEGFP and pDsRed2-Mito, and the merged fluorescence image is displayed.

(C) Cos-1 cells were transiently transfected with pEGFP-MLS and pDsRed2-Mito, and the merged images of green and red fluorescence are shown. Yellow evidences colocalization of both proteins.

(D–F) HeLa cells were transiently transfected with pEGFP-MLS and pDsRed2-Mito, and (D) the red fluorescence, (E) the green fluorescence, (F) and the merged images showing colocalization are displayed.

(G) HeLa cell transiently transfected with pEGFP-M1-H1, the construct with the full-length RNase H1 fused to the GFP.

(H) HeLa cell transiently transfected with pEGFP-M27-H1, the construct missing the MLS sequence from RNase H1. All cells were observed 24 hr after transfection using a Bio-Rad confocal microscope.

By E9.5, mitochondrial function is markedly compromised in *Rnaseh1*$^{-/-}$ embryos, as shown by the absence of cytochrome c oxidase activity (Figure 4). Mitochondrial dysfunctions are well-known inducers of apoptotic cell death, and mitochondria of *Rnaseh1*$^{-/-}$ embryos display the characteristic morphology of organelles programmed to trigger apoptosis (Scorrano et al., 2002). Mitochondrial remodeling results in release of cytochrome c, which in turn induces the postmitochondrial apoptotic pathway. *Rnaseh1*$^{-/-}$ embryos undergo massive apoptosis at day E9.5 (Figure 5).

Mice deleted for mitochondrial transcription factor A (mtTFA) (Larsson et al., 1998) or cytochrome c (Li et al., 2000) arrest development at the same stage as the *Rnaseh1* null mice. Notably, *Rnaseh1*$^{-/-}$ and *Tfam*-defective embryos exhibit significant apoptosis, whereas *cyc1*$^{-/-}$ embryos have been reported to be resistant to several proapoptotic effects (Li et al., 2000). Cell lines have been derived from cytochrome c-defective embryos but not from either *Tfam* (Wang et al., 2001) or *Rnaseh1* null mice (data not shown). A common mechanism for induction of apoptosis in *Rnaseh1*- and *Tfam* null embryos may be loss of mitochondrial membrane integrity and subsequent release of cytochrome c. The absence of cytochrome c in the *cyc1* null embryos may account for the success in obtaining stable fibroblast cell lines from these mice but not from *Rnaseh1*$^{-/-}$ or *Tfam*$^{-/-}$ embryos.

Although previous reports have suggested mitochondrial localization, our data conclusively establish that mouse RNase H1 has an N-terminal MLS capable of targeting the protein to mitochondria (Figure 6). The MLS is located between two in-frame AUG codons, and the choice of which AUG is used for translation can be dictated either by alternative splicing of pre-mRNA or leaky scanning translation of a single mRNA (Neupert, 1997). Our localization experiments used the cDNA sequence starting at the first AUG codon fused to the CMV promoter sequence, suggesting that leaky scanning of a single mRNA accounts for the relative amounts of GFP-RNase H1 fusion proteins detected in the nucleus and mitochondria.

Human DNA topoisomerase IIIα is an example of a protein directed to both nuclear and mitochondria sub-

cellular compartments by alternative translation initiation (Wang et al., 2002). Two in-frame AUGs of the h*TOP3*α mRNA are arranged similarly to the ones in the *Rnaseh1* mRNA. Until recently, hTop3α was thought to be exclusively a nuclear enzyme. However, the MLS sequence with an optimal translation initiation site was able to direct a GFP fusion protein to mitochondria. Subcellular partitioning of RNase H1 was similar to that of the Top3α, with the majority of both proteins residing in the nucleus (Wang et al., 2002). This distribution seems to be common for proteins that interact with DNA in both nuclei and mitochondria and is thought to be a way to ensure a proper ratio protein-DNA, since there is roughly 100-fold more DNA in the mammalian nucleus than in the mitochondria of these cells (Shadel and Clayton, 1997).

Our results suggest significant participation of RNase H1 in mitochondrial biogenesis. RNase H1 was not considered until now as a mitochondrial component critical for maintenance of mtDNA, and in the asymmetric strand replication model, its role was relegated to removal of RNA primers attached to DNA, which are used only for initiation of replication from the H and L strand. The presence of RNA at 500 bp intervals around the entire nonreplicating mtDNA (Yang et al., 2002) could not be the consequence of RNA left over from H and L strand primers. Although RNases H have been shown to participate in Okazaki fragment primer removal, other enzymes are necessary to completely eliminate all RNA residues (Rumbaugh et al., 1999), because RNases H leave one or more ribonucleotides attached to the DNA. In light of our results, we propose that RNase H1 is involved in removal of RNA during maturation of mtDNA, leaving ribonucleotides scattered throughout the DNA (Figure 7).

Replicating mtDNA molecules (Yang et al., 2002) contain even more extensive RNA regions, suggesting that priming events occur frequently during replication, as in the lagging strand of the strand-couple mechanism of DNA replication. Persistence of these hybrids suggests that RNase H1 removes them slowly, perhaps due to its low abundance or its presence in a complex whose function is not solely to resolve RNA-DNA hybrids. For example, RNase H1 may play a significant role in generating primers for DNA replication (Figure 7) as it does in ColE1 replication in *E. coli* (Dasgupta et al., 1987) or in HIV-1 where RNase H generates the RNA primers for initiation of second-strand synthesis (Hughes et al., 1998). Inability to generate RNA primers would clearly result in no or abortive replication.

During our analysis of embryonic lethality of *Rnaseh1*$^{-/-}$ mice, it was reported that RNase H1 is required for metamorphosis in *Drosophila melanogaster* (Filippov et al., 2001). The unique requirement for RNase H1 during development suggests to us that this enzyme is important in multicellular organisms when rapid mtDNA replication is necessary. Prompt removal of the RNA-DNA hybrids might be critical at the time of rapid mtDNA formation, making RNase H1 essential. Replication in somatic cells may be slow and tolerate the presence of a significant number of ribonucleotides in the mtDNA molecule, as reported (Yang et al., 2002), explaining the dispensability of RNase H1 in a number of unicellular organisms (Ray and Hines, 1995).

Participation of RNase H1 in mitochondrial biogenesis has implications for human mitochondrial dysfunctions and for HIV-AIDS. It will be of interest to see if RNase H1 plays an important role in mitochondrial diseases. RNase H of HIV-1 exhibits similarity in structure and enzymatic mechanism to *E. coli* RNase HI and to mammalian RNases H1 (Hughes et al., 1998). In light of our findings, efforts underway to develop drugs targeted to the HIV-1 RNase H for controlling HIV-AIDS should focus primarily on inhibition of the viral protein.

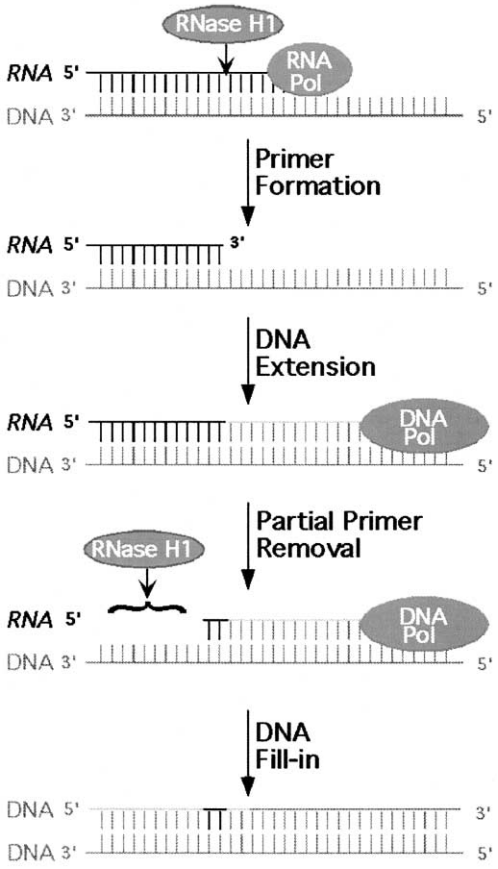

Figure 7. RNase H1 Involvement in Replication of Mitochondrial DNA

Putative roles of RNase H1 during mtDNA replication. Lagging-strand DNA synthesis originates from an RNA primer. RNase H1 cleaves a nascent RNA transcript to create primers for DNA formation. After DNA extension, RNase H1 removes the RNA primer, leaving a few nucleotides attached to the DNA molecule. After DNA polymerase γ synthesis and ligation, mtDNA would contain ribonucleotides dispersed throughout the entire molecule, as has been observed in a recent paper (Yang et al., 2002).

Experimental Procedures

Construction of the Targeting Vector

A BAC plasmid containing the mouse *Rnaseh1* (Cerritelli and Crouch, 1998) was sequenced and used for the construction of the targeting vector. A 2.2 kb of 5′-flanking sequence including most of the first exon and intron, and a 1.7 kb of 3′-flanking region consisting of exons 6, 7, and 8 and the intervening introns, were cloned flanking the neomycin resistance cassette of the plasmid X-pPNT (Tybulewicz et al., 1991) which also includes a thymidine kinase marker (Figure 1A). The final construct was verified by restriction digestion, PCR, and partial sequence determination.

Generation of Knockout Mice

Linearized targeting vector was electroporated into mouse ES cells derived from the 129SVJ strain (Fisher et al., 1998). ES clones resistant to G418 and sensitive to Gancyclovir were picked and screened for the targeted *Rnaseh1* allele by Southern analysis. Three clones containing the deleted gene were obtained and confirmed through a second round of screening. Two of the positive ES clones were injected into blastocyst derived from C57/BLK6 mice. Mice carrying the targeted allele in the germline were established, and heterozygous animals were mated to generate *Rnaseh1*$^{-/-}$ embryos.

Genotyping

ES cells that generated mice with the *Rnaseh1* gene deleted were screened by Southern analysis. Probes outside the region cloned in the targeting vector were used to detect wild-type and deleted band, as illustrated in Figure 1B. Mice offspring and embryos were screened by PCR and in some instances confirmed by Southern analysis. Competitive PCR was used to assess the presence of the wild-type and deleted alleles in the same reaction. An oligo primer for the neomycin gene (5′-CTTGCTCCTGCCGAGAAAGT) and a primer for the wild-type gene (5′-CCATCATGCAAGCCAAGGCT) were amplified with a downstream primer common for both alleles (5′-CTGAGTGAGCTCGTCCAGCT). The PCR products were analyzed in agarose gel (Figure 1C) and further verified by subcloning and sequencing. When working with small amount of embryonic tissue, primers that produced smaller products, and separated PCR reactions for wild-type and deleted allele were used. The PCR products were also confirmed by DNA sequence determination.

Mouse Embryo Analysis

Embryos from timed pregnancies were isolated and photographed using a dissecting microscope. Yolk sac or small pieces of embryos were used for genotyping by PCR. Embryos were fixed in 10% formalin, embedded in paraffin, sectioned, and stained with hematoxylin and eosin (H&E).

Quantitative PCR

Quantitative PCR was performed using the Light-Cycler system (Roche Molecular System). The PCR was monitored in real time with SYBR Green I dye, which binds preferentially to double-stranded DNA (Wittwer et al., 1997) and allows detection of PCR products as they are made. The higher the starting quantity of template, the earlier a significant increase in fluorescence is observed (Bieche et al., 1999). For wild-type and mutant embryos, the amount of mtDNA was determined using primers Co1F (5′-CCCAATCTCTACCAG CATC) and Co1R (5′-GGCTCATAGTATAGCTGGAG) of the cytochrome c oxidase subunit I (*mt-Co1*). The amount of chromosomal DNA was estimated with primers for H19 1 (2762 Forward 5′-GTACC CACCTGTCGTCC) and 2 (2948 Reverse 5′-GTCCACGAGACCAAT GACTG). The amount of T cell receptor ζ chain was estimated using primers Z3 (AAGGACGATCTGAGTACTGAG) and 150 (GAAGAGAG GAATATGACGTCTTGGAGAAGA). Calibration curves for mitochondrial and chromosomal genes were constructed from serial dilutions of DNA from wild-type embryos and were used to determine the amount of *mt-Co1*, H19 Spretus, and T cell receptor ζ chain genes in mutant embryos. The amount of mitochondrial DNA was then divided by the amount of the chromosomal DNA to obtain a normalized value.

Morphological and Biochemical Analysis

Electron microscopy and enzyme histochemistry were performed as described previously (Larsson et al., 1996, 1997). TUNEL assays were performed as described by the supplier of the TACS•XL-DAB kit (Trevigen, Inc., Gaithersburg, MD).

Cellular Localization

The sequence corresponding to the first 26 amino acids of RNase H1, containing the putative mitochondrial localization signal, was introduced into the multiple cloning site of plasmid pEGFP-N2 (Clontech) in frame with the ATG codon of the GFP gene, producing the plasmid pEGFP-MLS. Similarly, plasmid pEGFP-M1-H1 was generated by cloning the complete cDNA sequence of the *Rnaseh1* gene into the same region of the pEGFP-N1, and plasmid pEGFP-M27-H1 was constructed in the same way but using the RNase H1 coding sequence starting at M27, which should remove the mitochondrial localization signal.

To study intracellular localization of the various GFP-RNase H1 fusion proteins, the expression plasmids were transfected into African green monkey kidney-derived Cos-1 cells or HeLa cells that had been grown on coverslips. The plasmid pDsRed2-Mito (Clontech) was cotransfected with some constructs in some experiments to label the mitochondrial compartment with red fluorescence. Cells were allowed to grow for 24 hr in growth medium prior to analysis by confocal microscopy.

Acknowledgments

We thank Mahua Mukhopadhyay and Heiner Westphal for providing *Ldb1*$^{-/-}$ embryos and results prior to publication, Susan Mackem for teaching us to dissect embryos from decidua, and Sing Ping Huang for providing feeder cells for growth of ES cells. Marat Gorivodsky was very helpful for staging mouse embryos. Also, our thanks to Karl Pfieffer and Mario Cerritelli for help with the manuscript and figures.

Received: September 18, 2002
Revised: December 13, 2002

References

Arudchandran, A., Cerritelli, S., Narimatsu, S., Itaya, M., Shin, D.Y., Shimada, Y., and Crouch, R.J. (2000). The absence of ribonuclease H1 or H2 alters the sensitivity of *Saccharomyces cerevisiae* to hydroxyurea, caffeine and ethyl methanesulphonate: implications for roles of RNases H in DNA replication and repair. Genes Cells *5*, 789–802.

Bieche, I., Onody, P., Laurendeau, I., Olivi, M., Vidaud, D., Lidereau, R., and Vidaud, M. (1999). Real-time reverse transcription-PCR assay for future management of ERBB2-based clinical applications. Clin. Chem. *45*, 1148–1156.

Cazenave, C., Frank, P., Toulmé, J.J., and Büsen, W. (1994). Characterization and subcellular-localization of ribonuclease H activities from *Xenopus laevis* oocytes. J. Biol. Chem. *269*, 25185–25192.

Cerritelli, S.M., and Crouch, R.J. (1998). Cloning, expression, and mapping of ribonucleases H of human and mouse related to bacterial RNase HI. Genomics *53*, 300–307.

Chase, J.W., and Dawid, I.B. (1972). Biogenesis of mitochondria during *Xenopus laevis* development. Dev. Biol. *27*, 504–518.

Clayton, D.A. (1982). Replication of animal mitochondrial DNA. Cell *28*, 693–705.

Crouch, R.J., Arudchandran, A., and Cerritelli, S.M. (2001). RNase H1 of *Saccharomyces cerevisiae*: methods and nomenclature. Methods Enzymol. *341*, 395–413.

Crouch, R.J., and Toulmé, J.J. (1998). Ribonucleases H (Paris: INSERM).

Dasgupta, S., Masukata, H., and Tomizawa, J. (1987). Multiple mechanisms for initiation of ColE1 DNA replication: DNA synthesis in the presence and absence of ribonuclease H. Cell *51*, 1113–1122.

de Massy, B., Fayet, O., and Kogoma, T. (1984). Multiple origin usage for DNA replication in sdrA(rnh) mutants of *Escherichia coli* K-12. Initiation in the absence of oriC. J. Mol. Biol. *178*, 227–236.

Ebert, K.M., Liem, H., and Hecht, N.B. (1988). Mitochondrial-DNA in the mouse preimplantation embryo. J. Reprod. Fertil. *82*, 145–149.

Engel, M.L., Hines, J.C., and Ray, D.S. (2001). The *Crithidia fasciculata* RNH1 gene encodes both nuclear and mitochondrial isoforms of RNase H. Nucleic Acids Res. *29*, 725–731.

Filippov, V., Filippova, M., and Gill, S.S. (2001). *Drosophila* RNase H1 is essential for development but not for proliferation. Mol. Genet. Genomics *265*, 771–777.

Fisher, C.R., Graves, K.H., Parlow, A.F., and Simpson, E.R. (1998). Characterization of mice deficient in aromatase (ArKO) because of targeted disruption of the cyp19 gene. Proc. Natl. Acad. Sci. USA *95*, 6965–6970.

Frank, P., Braunshofer-Reiter, C., Poltl, A., and Holzmann, K. (1998a). Cloning, subcellular localization and functional expression of human RNase HII. Biol. Chem. *379*, 1407–1412.

Frank, P., Braunshofer-Reiter, C., and Wintersberger, U. (1998b). Yeast RNase H(35) is the counterpart of the mammalian RNase HI, and is evolutionarily related to prokaryotic RNase HII. FEBS Lett. *421*, 23–26.

Ginsberg, L., and Hillman, N. (1973). ATP metabolism in cleavage-staged mouse embryos. J. Embryol. Exp. Morphol. *30*, 267–282.

Holt, I.J., Lorimer, H.E., and Jacobs, H.T. (2000). Coupled leading- and lagging-strand synthesis of mammalian mitochondrial DNA. Cell *100*, 515–524.

Hughes, S.H., Arnold, E., and Hostomsky, Z. (1998). RNase H of retroviral reverse transcriptase. In Ribonucleases H, R.J. Crouch and J.J. Toulmé, eds. (Paris: INSERM), pp. 195–224.

Itaya, M., Omori, A., Kanaya, S., Crouch, R.J., Tanaka, T., and Kondo, K. (1999). Isolation of RNase H genes that are essential for growth of *Bacillus subtilis* 168. J. Bacteriol. *181*, 2118–2123.

Kogoma, T., and Foster, P.L. (1998). Physiological functions of *E. coli* RNase HI. In Ribonucleases H, R.J. Crouch and J.J. Toulmé, eds. (Paris: INSERM), pp. 39–66.

Lakshmipathy, U., and Campbell, C. (1999). The human DNA ligase III gene encodes nuclear and mitochondrial proteins. Mol. Biol. Cell *19*, 3869–3876.

Larsson, N.G., Garman, J.D., Oldfors, A., Barsh, G.S., and Clayton, D.A. (1996). A single mouse gene encodes the mitochondrial transcription factor A and a testis-specific nuclear HMG-box protein. Nat. Genet. *13*, 296–302.

Larsson, N.G., Oldfors, A., Garman, J.D., Barsh, G.S., and Clayton, D.A. (1997). Down-regulation of mitochondrial transcription factor A during spermatogenesis in humans. Hum. Mol. Genet. *6*, 185–191.

Larsson, N.G., Wang, J., Wilhelmsson, H., Oldfors, A., Rustin, P., Lewandoski, M., Barsh, G.S., and Clayton, D.A. (1998). Mitochondrial transcription factor A is necessary for mtDNA maintenance and embryogenesis in mice. Nat. Genet. *18*, 231–236.

Lee, D.Y., and Clayton, D.A. (1997). RNase mitochondrial RNA processing correctly cleaves a novel R loop at the mitochondrial DNA leading-strand origin of replication. Genes Dev. *11*, 582–592.

Lee, D.Y., and Clayton, D.A. (1998). Initiation of mitochondrial DNA replication by transcription and R-loop processing. J. Biol. Chem. *273*, 30614–30621.

Li, K., Li, Y.C., Shelton, J.M., Richardson, J.A., Spencer, E., Chen, Z.J., Wang, X.D., and Williams, R.S. (2000). Cytochrome c deficiency causes embryonic lethality and attenuates stress-induced apoptosis. Cell *101*, 389–399.

Mukhopadhyay, M., Teufel, A., Yamashita, T., Agulnik, A.D., Chen, L., Downs, K.M., Schindler, A., Grinberg, A., Huang, S.P., and Westphal, H. (2003). Functional ablation of the mouse Ldb1 gene results in severe patterning defects during gastrulation. Development *130*, 495–505.

Nakai, K., and Horton, P. (1999). PSORT: a program for detecting sorting signals in proteins and predicting their subcellular localization. Trends Biochem. Sci. *24*, 34–36.

Neupert, W. (1997). Protein import into mitochondria. Ann. Rev. Biochem. *66*, 863–917.

Pikó, L., and Matsumoto, L. (1977). Complex forms and replicative intermediates of mitochondrial DNA in tissues from adult and senescent mice. Nucleic Acids Res. *4*, 1301–1314.

Pikó, L., and Taylor, K.D. (1987). Amounts of mitochondrial DNA and abundance of some mitochondrial gene transcripts in early mouse embryos. Dev. Biol. *123*, 364–374.

Pileur, F., Toulmé, J.J., and Cazenave, C. (2000). Eukaryotic ribonucleases HI and HII generate characteristic hydrolytic patterns on DNA-RNA hybrids: further evidence that mitochondrial RNase H is an RNase HII. Nucleic Acids Res. *28*, 3674–3683.

Ray, D.S., and Hines, J.C. (1995). Disruption of the *Crithidia fasciculata* RNH1 gene results in the loss of two active forms of Ribonuclease H. Nucleic Acids Res. *23*, 2526–2530.

Rumbaugh, J.A., Henricksen, L.A., DeMott, M.S., and Bambara, R.A. (1999). Cleavage of substrates with mismatched nucleotides by Flap endonuclease-1. Implications for mammalian Okazaki fragment processing. J. Biol. Chem. *274*, 14602–14608.

Scorrano, L., Ashiya, M., Buttle, K., Weiler, S., Oakes, S.A., Mannella, C.A., and Korsmeyer, S.J. (2002). A distinct pathway remodels mitochondrial cristae and mobilizes cytochrome c during apoptosis. Dev. Cell *2*, 55–67.

Shadel, G.S. (1999). Yeast as a model for human mtDNA replication. Am. J. Hum. Genet. *65*, 1230–1237.

Shadel, G.S., and Clayton, D.A. (1997). Mitochondrial DNA maintenance in vertebrates. Ann. Rev. Biochem. *66*, 409–435.

Slusher, L.B., Gillman, E.C., Martin, N.C., and Hopper, A.K. (1991). mRNA leader length and initiation codon context determine alternative AUG selection for the yeast gene MOD5. Proc. Natl. Acad. Sci. USA *88*, 9789–9793.

Stein, H., and Hausen, P. (1969). Enzyme from calf thymus degrading the RNA moiety of DNA-RNA Hybrids: effect on DNA-dependent RNA polymerase. Science *166*, 393–395.

Steuerwald, N., Barritt, J.A., Adler, R., Malter, H., Schimmel, T., Cohen, J., and Brenner, C.A. (2000). Quantification of mtDNA in single oocytes, polar bodies and subcellular components by real-time rapid cycle fluorescence monitored PCR. Zygote *8*, 209–215.

ten Asbroek, A.L.M.A., van Groenigen, M., Nooij, M., and Baas, F. (2002). The involvement of human ribonucleases H1 and H2 in the variation of response of cells to antisense phosphorothioate oligonucleotides. Eur. J. Biochem. *269*, 583–592.

Tybulewicz, V., Tremblay, M.L., Lamarca, M.E., Stubblefield, B.K., Winfield, S., Zablock, B., Sidransky, E., Martin, B.M., Westphal, H., Mulligan, R.C., and Ginns, E.I. (1991). Generation of chimeric mice with glucocerebrosidase gene mutations introduced by targeted homologous recombination in embryonic stem cells to produce a mouse model of Gaucher disease. Am. J. Hum. Genet. *49*, 441.

Valgardsdottir, R., Brede, G., Eide, L.G., Frengen, E., and Prydz, H. (2001). Cloning and characterization of MDDX28, a putative DEAD-box helicase with mitochondrial and nuclear localization. J. Biol. Chem. *276*, 32056–32063.

Wang, H., and Lambowitz, A.M. (1993). Reverse transcription of the Mauriceville plasmid of Neurospora - lack of ribonuclease H activity associated with the reverse transcriptase and possible use of mitochondrial ribonuclease H. J. Biol. Chem. *268*, 18951–18959.

Wang, J.M., Silva, J.P., Gustafsson, C.M., Rustin, P., and Larsson, N.G. (2001). Increased in vivo apoptosis in cells lacking mitochondrial DNA gene expression. Proc. Natl. Acad. Sci. USA *98*, 4038–4043.

Wang, Y., Lyu, Y.L., and Wang, J.C. (2002). Dual localization of human DNA topoisomerase III alpha to mitochondria and nucleus. Proc. Natl. Acad. Sci. USA *99*, 12114–12119.

Wittwer, C.T., Ririe, K.M., Andrew, R.V., David, D.A., Gundry, R.A., and Balis, U.J. (1997). The LightCycler(TM) a microvolume multisample fluorimeter with rapid temperature control. Biotechniques *22*, 176–181.

Yang, M.Y., Bowmaker, M., Reyes, A., Vergani, L., Angeli, P., Gringeri, E., Jacobs, H.T., and Holt, I.J. (2002). Biased incorporation of ribonucleotides on the mitochondrial L-strand accounts for apparent strand-asymmetric DNA replication. Cell *111*, 495–505.